Strong dispersive effects in the light-scattering mean free path in photonic gaps

P. D. García,[*] R. Sapienza, L. S. Froufe-Pérez, and C. López

Instituto de Ciencia de Materiales de Madrid (CSIC) and Unidad Asociada CSIC-UVigo, Cantoblanco, 28049 Madrid, Spain
(Received 9 June 2009; published 30 June 2009)

We have performed measurements of the scattering mean free path (ℓ_s) in photonic crystals with different and controlled amounts of disorder. In the most perfect crystals, 1 order of magnitude chromatic variation in ℓ_s for just 3% shift around the band gap (27 nm in wavelength) is obtained. It is argued that the ℓ_s dispersion is governed by both the total density of states and the group index in the incident direction, with this last quantity being responsible for the large dispersion of ℓ_s.

The ability to modify and enhance light scattering in disordered systems is much sought after. Artificially engineered materials allow the control of light transport and density of light states $N(\omega)$ through interference in the internal nanostructure rather than on the refraction in the body boundaries, engendering new materials properties. Photonic crystals in which the dielectric constant is periodically modulated control fundamental aspects of light-matter interaction such as light emission[1] and light transport,[2] much like semiconductors controlling electrons. Redistribution and inhibition of the emission from photonic crystals were proven,[3] but unconventional light transport in partially disordered photonic crystals has only been hinted at by pioneering experiments.[4] Other topologies, such as random media,[5,6] correlated disordered,[7] or fractal,[8] employ the aperiodic subwavelength dielectric nanostructure to achieve similar light control for transport[9] and random lasing emission.[10]

Light scattering by weak topological disorder in a photonic crystal and interplay between order and disorder has yet to be fully understood and explored. As an important step, the relation between scattering extinction and $N(\omega)$ has just been theoretically derived.[11] As pointed out by John[2] a dramatic change in light diffusion can occur for frequencies in or around the band gap and eventually Anderson localization of light can be reached, with the photonic conductor becoming an insulator.[12] In the quest for light localization, the first experiments focused on fully random media[13] and only recently has transverse localization been reported in two-dimensional crystals with disorder.[14]

Even far from the localization regime, the scattering properties of Bloch modes, the periodic electromagnetic modes of a photonic crystal, are expected to be profoundly different from the diffusive modes encountered in conventional random media. Pioneering experiments on coherent backscattering[15] and diffuse light transport[16,17] in photonic crystals searched for signatures of Bloch-mode mediated scattering but have merely shown standard light diffusion.[18]

In this Rapid Communication we study the scattering mean free path, ℓ_s, the fundamental building block for any wave transport model, for the special case of photonic crystals with a controlled amount of disorder. We report experimental evidence of strong chromatic dispersion of ℓ_s from band edge to band gap, tightly linked to the reduced density of states,[19] and values of up to $\sim 100-500$ μm, i.e., ~ 300 times the lattice parameter (a), an order of magnitude higher than previously reported,[15–17] and in a spectral region where the total density of states has just a hardly visible feature.

Single scattering events in a system with modified light modes and density of states, as in a photonic crystal, are expected to be very different from those occurring in vacuum due to: (a) an increase in light-matter interaction and thus of scattering by defects when $N(\omega)$ is increased at the vicinity of band edges and (b) a suppression of the scattering channels, i.e., a increase in ℓ_s in the band gap, where $N(\omega)$ is strongly reduced.

The scattering strength can be studied via simultaneous reflection and transmission measurements, when absorption is negligible [the absorption length $\ell_a \sim 10$ m (Ref. 20)], and for energies below the onset of diffraction ($a/\lambda \sim 1.12$,[21] where λ is the light wavelength). We assume that scattering losses follow Lambert-Beer's law; i.e., after a thickness L, a ballistic beam attenuates as $I(L) = I_0 \exp(-L/\ell_s)$. The intensity balance can then be expressed as

$$T(L) + R(L) = \exp(-L/\ell_s), \qquad (1)$$

where $T(L)$ and $R(L)$ are the ballistic transmission and reflection as a function of sample thickness in a given direction.

The samples are polymethil-metacrilate (PMMA) (refractive index, $n = 1.49$) self-assembled fcc photonic crystals[22] with controlled density of intentionally added vacancies[7] (from 0% to 40%) [see Figs. 1(a) and 1(b)]. These vacancies are obtained upon removal of given fractions of constituting spheres from random lattice positions.

The scattering mean free path in a random medium can be shown to be $\ell_s = 1/\rho_s \sigma$, where σ is the scattering cross section and ρ_s is the scatterers number density.[9] ℓ_s is not only a measure of the quality of a photonic structure but also the basic length scale of a more complex picture of multiple scattering and light diffusion, meaning full regardless of the transport regime.

In our system, the degree of extrinsic disorder [see SEM images in Figs. 1(a) and 1(b)] can be very precisely and uniformly tuned while keeping the sample thickness controlled. This allows us to develop a setup to measure Lambert-Beer's law for photonic crystals. We used a Fourier-transform spectrometer coupled to a microscope allowing to probe the scattering in the (111) direction, with a small numerical aperture of 0.1 while illuminating a constant-thickness area with a spot of ~ 80 μm. The spectra [see Figs. 1(c) and 1(d)] are taken in adjacent regions, which are
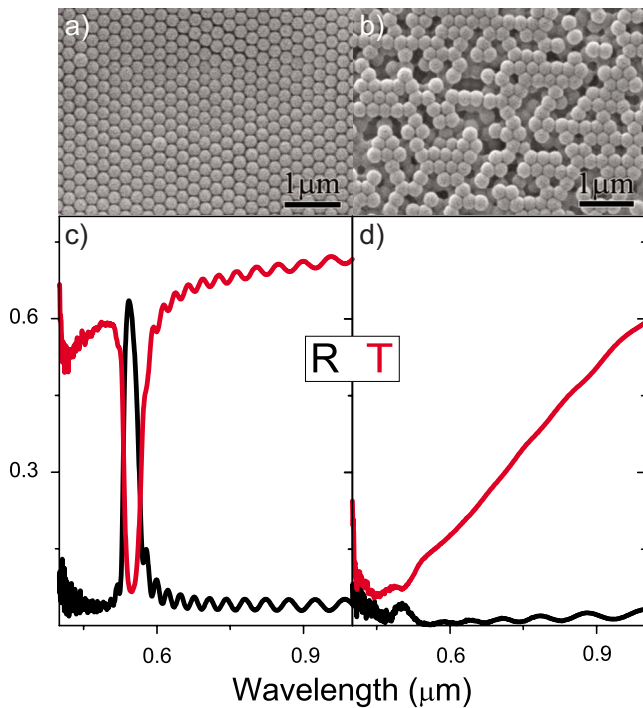
FIG. 1. (Color online) Top panel: Scanning electron microscopy (SEM) images of photonic crystal with (a) 0% and (b) 40% vacancy doping. (c) and (d) reflection and transmission from the corresponding samples of the above panel.

FIG. 3. (Color online) Figure shows ℓ_s as a function of the light wavelength for 0%, 10%, and 40% vacancy-doped photonic crystals with $d=237$ nm. The position of the pseudogap is shaded in gray. The dotted line shows the ω^{-2} dependence of ℓ_s far from the band gap.

visible by optical microscope inspection as terraces on the sample surface. The thickness of such layers is accurately measured with an uncertainty of 2%, via the density of Fabry-Pérot fringes visible in Fig. 1.

Figure 2(a) shows the measured $\ln(T+R)$ for three different degrees of vacancy doping,[7] i.e., for different degrees of extrinsic disorder, at a wavelength of 633 nm and for spheres of 237 nm in diameter ($a/\lambda=0.52$). In this type of represen-
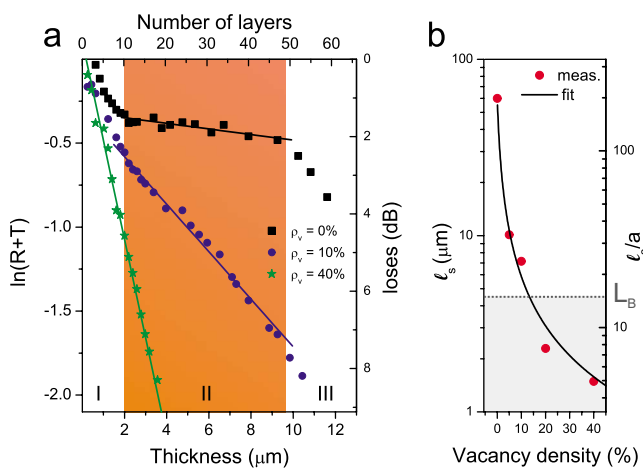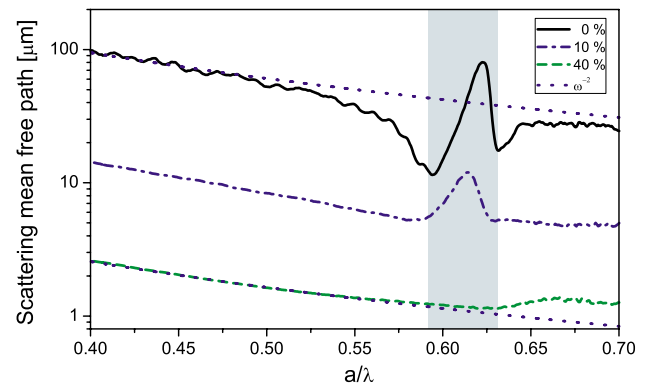

FIG. 2. (Color online) (a) Plot of $\ln(R+T)$ as a function of the sample thickness at $\lambda=633$ nm for different vacancy-density-doped photonic crystals (from 0% to 40% vacancy dopings) of 237 nm diameter. (b) ℓ_s obtained from linear fitting of the slope for regime II. It also shows the Bragg length (L_B) in the case of $\rho_v=0\%$ as shaded area.

tation, the slope yields directly $(-\ell_s)^{-1}$ according to Eq. (1). This wavelength is chosen to exemplify a spectral region at low energy where no photonic band features are present. In Fig. 2(a) three scattering regimes are clearly distinguishable. For thicknesses lower than ca. ten layers (regime I) up to $\sim$25–30 % of the incident light is scattered due to surface effects in the form of stacking patterns,[23] high lattice displacements, and even stacking order arrangements.[24] When the second regime (II) sets in, the slope ℓ_s^{-1} reaches a stationary value that characterizes the photonic crystal. Equation (1) holds and scattering losses scale with sample thickness such as $\sim\exp(L/\ell_s)$. Finally, for larger thicknesses, a third scattering regime (III) appears for thick samples >50 layers when the self-assembling process loses its effectiveness and cracks appear.

The physical picture we propose can be checked against consistency if additional disorder, in the form of a controlled concentration of vacancies, is added to the photonic crystals. At a wavelength of 633 nm the values of ℓ_s, calculated from the fit to the Lambert-Beer law, are plotted as a function of vacancy density in Fig. 2(b). The "perfect" crystal (that with 0% added vacancies) is highly ordered as it presents a scattering mean free path of 63 μm, hundreds of times the lattice constant (in this case $a=0.33$ μm), and in particular much larger than the Bragg length (of the thick sample)[25] that in our case is $L_B=(3.8\pm0.3)$ μm. An addition of a very small amount of defects rapidly decreases the mean free path and, hence, the quality of the crystal. In this figure, the inverse scattering mean free path scales linearly with the vacancy concentration ρ_v, as shown by the black line, which is a fit for $\ell_s^{-1}=\rho_0\sigma_0+\rho_v\sigma_v$, where ρ_0 and ρ_v are the density of intrinsic and intentionally added scatterers and σ_0 and σ_v are their scattering cross section, respectively. From the fit of $\ell_s(\rho_v)$ as a function of the vacancy concentration we can estimate $\sigma_v=(0.016\pm0.002)$ μm^2.

Figure 3 shows the strong chromatic dispersion of $\ell_s(\omega)$ in the visible range. This is the signature of the photonic crystal. In the low-energy side of the pseudobandgap, ℓ_s takes on a value on the order of $\sim$100 μm for sphere diameter $d=237$ nm and $\sim$500 μm for $d=600$ nm (not shown

here), the largest values reported so far. Previous experiments[15–17] have measured ℓ_t, the transport mean free path, from very thick (~ 200 μm) photonic crystals grown by natural sedimentation[16,17] or centrifugation[15] and found values in the range of $7 < \ell_t < 20$ μm. ℓ_s is in general smaller than ℓ_t, and therefore the values found in our experiment represent a much higher degree of ordering than previous reports. Far from the band gap, $\ell_s(\omega)$ varies as $\sim \omega^{-2}$, a dependence that has been confirmed also in previous experiments[15] and attributed to Rayleigh-Gans type of scattering.

Surprisingly, near a gap, the large variation in ℓ_s cannot be attributed to the modified density of states only. The scattering cross section (σ) of a scatterer immersed in a finite structure is the ratio of the total radiated power by the scatterer to the incoming intensity impinging into the system. Two processes contribute hence to the scattering of light: the incoming signal coupling to the scatterer and the polarized scatterer coupling to the radiative electromagnetic field modes. The strength of the latter coupling is accounted for by the local density of states $\rho(\omega, \mathbf{r})$ at the scatterer position, whose spatial average is the density of states $N(\omega)$,[27,28] while the former is instead accounted for by the group index $n_g(\omega, \mathbf{k})$.[29] $n_g(\omega, \mathbf{k})$ of the finite crystal is proportional to the spectral function $S(\omega, \mathbf{k})$ of the system,[26–28] which describes the number of states available for the vacuum-crystal coupling of a signal in direction $\mathbf{k}$, with frequency ω. This simple heuristic model breaks down at high energies, where propagation through a unique k vector is not possible or in regions where $\rho(\omega, \mathbf{r})$ undergoes strong variations and the spatial average procedure is not anymore justified.

With the above considerations, the scattering cross section, in the Rayleigh limit, of a scatterer in a photonic crystal can therefore be described by

$$\sigma_{\mathbf{k}}(\omega) \propto F(\omega)\omega^2 N(\omega) n_g(\omega, \mathbf{k}), \qquad (2)$$

where $F(\omega)$ is a form factor that takes into account corrections beyond Rayleigh scattering. In our simple model, the form factor can be replaced by a Rayleigh-Gans factor $F(\omega) \sim \omega^{-2}$ and the polarizability of the scatterer can be considered as independent of frequency.[15]

The dependence on $n_g(\omega, \mathbf{k})$ typically disappears in ordinary random media for which the photonic modes are isotropic and energetically smooth but is very important for the Bloch modes of photonic crystals. At the band edges of our photonic crystals, $\ell_s(\omega)$ has a sharp decrease in a factor of up to 4, $\ell_s(a/\lambda = 0.59) = 11 \pm 1$ μm, and then it shoots up almost an order of magnitude in the band gap to $\ell_s(a/\lambda = 0.62) = 81 \pm 40$ μm. Such an eightfold increase occurs within just 0.03 in a/λ and ~ 27 nm in wavelength, around the photonic band gap. Again, as a comparison, we show in Fig. 3 the frequency dependence of ℓ_s for the 10% and the 40% vacancy photonic crystal; the latter can be considered fully disordered. As the vacancy doping is increased, the profile is smoothed. First the band-edge effect on ℓ_s disappears as these standing-wave-like states are very sensitive to disorder. Then, for the 40% vacancy case, the effects on $N(\omega)$ and n_g are washed out and the only feature in ℓ_s occurs at the position of the first Mie resonance of the individual
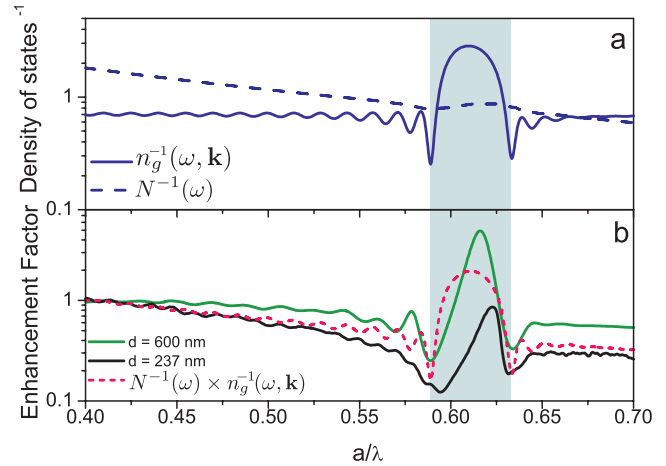

FIG. 4. (Color online) (a) Inverse of the total $N(\omega)$ density of states and group index $n_g[\omega, \mathbf{k} = (1,1,1)]$ along the incident direction (Γ-L direction) are plotted. (b) Enhancement factor, $\ell_s(a/\lambda)/\ell_s(a/\lambda = 0.4)$, for two opals with no vacancy doping and the quantity $N^{-1}(\omega)n_g^{-1}[\omega, \mathbf{k} = (1,1,1)]$. The position of the pseudogap is shaded in gray.

dielectric spheres.[20] This weak energy dependence of ℓ_s is likely to be the only residual effect in a very disordered opal as those grown by natural sedimentation or centrifugation,[15–17] which present superficial iridescence but are largely bulk disordered and exhibit standard light diffusion.

Figure 4(a) shows the inverse of the total density of states (dark blue dashed line) that has a very weak modulation at the gap together with $n_g^{-1}(\omega, \mathbf{k})$ for propagation parallel to $\mathbf{k} = (111)$ that does have a strong variation in the gap (violet full line). $n_g(\omega, \mathbf{k})$ is obtained from Ref. 29.

Figure 4(b) shows the enhancement factor defined as the ratio of ℓ_s to its value far from the gap, $\ell_s(a/\lambda)/\ell_s(a/\lambda = 0.4)$, for two different samples composed by PMMA spheres of 237 (black curve) and 600 nm (green/gray curve) in diameter, respectively. The enhancement factor points out the existence of a photonic pseudogap and reveals the variation in the density of states of the photonic crystal. A clear resonant behavior is evident. The variation in ℓ_s is eightfold for $d = 237$ nm and 20-fold for $d = 600$ nm, which we attribute to the superior quality of the lattice. In Fig. 4(b) we plot also $n_g^{-1}[\omega, \mathbf{k} = (1,1,1)]N(\omega)^{-1}$ (dashed pink curve) that, from Eq. (2), is expected to reproduce the shape of energy dependence of $\ell_s(\omega)$. A fair agreement between theory and experiment is obtained, and the qualitative behavior is well captured by our simple model. Although both $N(\omega)$ and $n_g(\omega, \mathbf{k})$ contribute to the strong variation in ℓ_s, it is evident that the principal factor responsible for a change in ℓ_s (111) is $n_g(\omega, \mathbf{k})$.

Our simple and qualitative model, despite being heuristic and limited to collinear propagation, accounts remarkably well for the shape of the measured $\ell_s(\omega)$, although it does not account for the asymmetry of its dispersion in the photonic gap. This effect is related to the available scattering states in other crystallographic directions close to the incident one.[30]

An increase of ℓ_s in the band gap and a decrease in the

band edge reflect the modified phase space available Δk for light scattering when the photonic modes are concentrated around few k directions or the available scattered states reduced. This is consistent with John's seminal prediction of a need for a modified Ioffe-Regel criterion[2] for scattering in photonic crystals to include Δk. Furthermore, here we show that as the phase space is modified, not only the Ioffe-Regel criterion is changed but also ℓ_s is renormalized: light scattering in photonic crystals is richer than in conventional amorphous media. Complete photonic band-gap materials, such as Si inverted opals, would amplify the effect here presented and could be proper candidates to observe Anderson localization of light.

In conclusion, we show that a controlled smooth transition from ballistic to diffuse transport in photonic crystals can be induced by the introduction of extrinsic disorder. We find that the strength of scattering is strongly determined by the spectral function, which induces immense, up to 20-fold, variations in the scattering mean free path. We propose ℓ_s as a robust, easy to measure, figure of merit in assessing the quality of photonic crystals for technological applications. The possibility of controlling light scattering and diffusion in nanostructured optical media has important implications not only in testing the quality of photonic devices but also in properly addressing the proximity to the onset of Anderson localization in disordered lattices or for the spectral control of lasing emission from disordered/ordered active media.[10]

*Present address: DTU Fotonik, Department of Photonics Engineering, Technical University of Denmark, Ørsteds Plads 343, DK-2800 Kgs. Lyngby, Denmark.

[1] E. Yablonovitch, Phys. Rev. Lett. **58**, 2059 (1987).

[2] S. John, Phys. Rev. Lett. **58**, 2486 (1987).

[3] P. Lodahl, A. F. van Driel, I. S. Nikolaev, A. Irman, K. Overgaag, D. Vanmaekelbergh, and W. L. Vos, Nature (London) **430**, 654 (2004); S. Noda, M. Fujita, and T. Asano, Nat. Photonics **1**, 449 (2007); A. F. Koenderink and W. L. Vos, Phys. Rev. Lett. **91**, 213902 (2003).

[4] C. Toninelli, E. Vekris, G. A. Ozin, S. John, and D. S. Wiersma, Phys. Rev. Lett. **101**, 123901 (2008).

[5] L. F. Rojas-Ochoa, J. M. Mendez-Alcaraz, J. J. Saenz, P. Schurtenberger, and F. Scheffold, Phys. Rev. Lett. **93**, 073903 (2004).

[6] P. Sheng, *Introduction to Wave Scattering, Localization, and Mesoscopic Phenomena* (Academic Press, San Diego, 1995).

[7] P. D. García, R. Sapienza, Á. Blanco, and C. López, Adv. Mater. **19**, 2597 (2007).

[8] P. Barthelemy, J. Bertolotti, and D. S. Wiersma, Nature (London) **453**, 495 (2008).

[9] E. Akkermans and G. Montambaux, *Mesoscopic Physics of Electrons and Photons* (Cambridge University Press, Cambridge, 2007).

[10] D. S. Wiersma, Nat. Phys. **4**, 359 (2008); S. Gottardo, R. Sapienza, P. D. García, A. Blanco, D. S. Wiersma, and C. López, Nat. Photonics **2**, 429 (2008).

[11] R. Carminati and J. J. Saenz, Phys. Rev. Lett. **102**, 093902 (2009).

[12] P. W. Anderson, Phys. Rev. **109**, 1492 (1958).

[13] D. S. Wiersma, P. Bartolini, A. Lagendijk, and R. Righini, Nature (London) **390**, 671 (1997); M. Störzer, P. Gross, C. M. Aegerter, and G. Maret, Phys. Rev. Lett. **96**, 063904 (2006); A. A. Chabanov, M. Stoytchev, and A. Z. Genack, Nature (London) **404**, 850 (2000).

[14] T. Schwartz, G. Bartal, S. Fishman, and M. Segev, Nature (London) **446**, 52 (2007).

[15] A. F. Koenderink, M. Megens, G. van Soest, W. L. Vos, and A. Lagendijk, Phys. Lett. A **268**, 104 (2000); J. Huang, N. Eradat, M. E. Raikh, Z. V. Vardeny, A. A. Zakhidov, and R. H. Baughman, Phys. Rev. Lett. **86**, 4815 (2001).

[16] V. N. Astratov, V. N. Bogomolov, A. A. Kaplyanskii, A. V. Prokofiev, L. A. Samoilovich, S. M. Samoilovich, and Yu. A. Vlasov, Nuovo Cimento Soc. Ital. Fis., D **17**, 1349 (1995).

[17] Y. A. Vlasov, M. A. Kaliteevski, and V. V. Nikolaev, Phys. Rev. B **60**, 1555 (1999).

[18] A. F. Koenderink, A. Lagendijk, and W. L. Vos, Phys. Rev. B **72**, 153102 (2005).

[19] E. Pavarini, L. C. Andreani, C. Soci, M. Galli, F. Marabelli, and D. Comoretto, Phys. Rev. B **72**, 045102 (2005).

[20] R. Sapienza, P. D. Garcia, J. Bertolotti, M. D. Martin, A. Blanco, L. Vina, C. Lopez, and D. S. Wiersma, Phys. Rev. Lett. **99**, 233902 (2007).

[21] F. García-Santamaría, J. F. Galisteo-López, P. V. Braun, and C. López, Phys. Rev. B **71**, 195112 (2005).

[22] P. Jiang, J. F. Bertone, K. S. Hwang, and V. L. Colvin, Chem. Mater. **11**, 2132 (1999).

[23] X. Checoury, S. Enoch, C. López, and A. Blanco, Appl. Phys. Lett. **90**, 161131 (2007).

[24] N. Denkov, O. Velev, P. Kralchevski, I. Ivanov, H. Yoshimura, and K. Nagayama, Langmuir **8**, 3183 (1992).

[25] J. F. Galisteo-López, E. Palacios-Lidón, E. Castillo-Martínez, and C. López, Phys. Rev. B **68**, 115109 (2003).

[26] R. G. Newton, *Scattering Theory of Waves and Particles*, 2nd ed. (Springer-Verlag, New York, 1982).

[27] R. C. McPhedran, L. C. Botten, J. McOrist, A. A. Asatryan, C. M. de Sterke, and N. A. Nicorovici, Phys. Rev. E **69**, 016609 (2004).

[28] A. Lagendijk and B. A. van Tiggelen, Phys. Rep. **270**, 143 (1996).

[29] J. F. Galisteo-López, M. Galli, M. Patrini, A. Balestreri, L. C. Andreani, and C. López, Phys. Rev. B **73**, 125103 (2006).

[30] M. A. Kaliteevski, J. M. Martinez, D. Cassagne, and J. P. Albert, Phys. Rev. B **66**, 113101 (2002).